Corresponding Author: Professor Melike Lakadamyali,

Corresponding Author's Institution: ICFO-Institut de Ciencies Fotoniques

First Author: Nela Durisic, PhD

Order of Authors: Nela Durisic, PhD; Lara Laparra Cuervo; Melike Lakadamyali

Super-resolution nanoscopy is an enabling tool for biology

Multiple molecular states of super-resolution probes complicate image quantification

It's easy to misinterpret nanoscopy images if unaware of pitfalls in data analysis

Same probe appearing many times can lead to overcounting and artificial clustering

Failed photoactivation of a probe can lead to undercounting and missed events

We describe methods for overcoming these challenges to properly quantify images

Quantitative super-resolution microscopy: pitfalls and strategies for image analysis

Nela Durisic[1], Lara Laparra Cuervo[1], Melike Lakadamyali[1*]

[1] ICFO-Institut de Ciencies Fotoniques, Mediterranean Technology Park, Av. Carl Friedrich Gauss, 3, 08860, Castelldefels (Barcelona), Spain

[*] Correspondence should be sent to M.L.: melike.lakadamyali@icfo.es

Abstract

Super-resolution microscopy is an enabling technology that allows biologists to visualize cellular structures at nanometer length scales using far-field optics. To break the diffraction barrier, it is necessary to leverage the distinct molecular states of fluorescent probes. At the same time, the existence of these different molecular states and the photophysical properties of the fluorescent probes can complicate data quantification and interpretation. Here, we review the pitfalls in super-resolution data analysis that must be avoided for proper interpretation of images.

Introduction

The immense toolbox of fluorescence probes has enabled us to tag almost anything inside cells with high molecular specificity and in many colors. However, due to diffraction, the resolving power of an optical microscope was, until recently, limited to ~200 nm in the lateral and ~500 nm in the axial direction. This limitation obscured essential details at the nanometer length scales. Fortunately, diffraction limit has now been broken thanks to the development of super-resolution microscopy methods including stimulated emission depletion microscopy (STED) [1], saturated structured illumination microscopy (SSIM) [2], stochastic optical reconstruction microscopy (STORM) [3] and (fluorescence) photoactivated localization microscopy (PALM and fPALM) [4,5] among others. These methods are starting to enable near molecular-scale spatial resolution in biological imaging. The advent of "nanoscopy" has also brought the need for proper data analysis tools to quantify the super-resolution images. The quantitative information of interest can take several forms including characterization of image resolution, measure of nanostructure or nanocluster sizes, quantification of spatial (co)-organization of nanoclusters and "molecular counting" of protein numbers. The increased resolution imposes stringent conditions on data analysis and extra care must be taken to ensure that photophysical properties of the probes, labeling and imaging strategies used do not lead to misinterpretation of the data. As the nanoscopy field has progressed at a fast pace, several new methods have also been developed for "post-image" analysis. This review will focus on considerations one must be aware of while quantifying super-resolution images. The emphasis will be given to methods based on single molecule localization (such as STORM, PALM, fPALM) but similar points are often also important for quantifying STED images.

Basic principles

Super-resolution methods that rely on single molecule localization have been the subject of several recent reviews and for in depth information the reader is directed elsewhere [6-8]. Briefly, the image of a single molecule is referred to as the point spread function (PSF) of the microscope. Even though the size of the PSF is determined by diffraction, the molecule's position can be precisely localized by finding the center of the PSF [9]. To avoid the problem of overlapping PSFs in a densely labeled sample, it is necessary to control the number of molecules that are fluorescently active at any given time. This active control of fluorophore density was made possible by the discovery of photoswitchable fluorophores [10-12]. In super-resolution imaging, only a small subset of fluorophores is photoactivated at any given time such that their PSFs are non-overlapping and their positions can be precisely determined. Through iterative cycles of activation and de-activation, the positions of all the fluorophores can be precisely determined, and these positions can then be used to reconstruct a high resolution image of the underlying structure.

Photoswitchable probes

A wide range of probes such as fluorescent proteins, small organic fluorophores and quantum dots are available for super-resolution imaging with single molecule localization. These probes typically fall into two categories [13,14]: (i) reversibly photoswitchable probes that can be cycled many times between bright and dark states such as small organic fluorophores (e.g. Alexa 647) [15] or photochromic fluorescent proteins (e.g. Dronpa) [16] and (ii) irreversibly photoactivatable and photoconvertible probes (e.g. PA-GFP and mEos2) [10,17] . These different categories provide complementary advantages for super-resolution imaging. Reversible probes lead to smoother images since the same structure is sampled many times [15]. However, the uncertainty in each localization makes it impossible to identify which localizations arise from the same fluorophore, especially when samples are densely labeled, thus making quantification challenging. Therefore, proper care must be taken to account for probe photophysical effects when quantifying images as described below.

Image resolution

The spatial resolution in nanoscopy can be affected by several factors including localization precision, labeling density and probe size. The localization precision mainly depends on the number of photons emitted, as well as other factors such as background noise, and pixel size [9,18,19]. Labeling density can be a major limitation to achieve high spatial resolution. Low labeling densities can cause continuous structures to appear discontinuous or clustered, resulting in a loss of detail. According to the Nyquist criterion [15,20,21], the labeling density must be such that the distance between individual localizations in the resulting image is at least half of the desired resolution.

In practice, quantifying the final image resolution can be quite difficult. While the localization precision alone can be analytically calculated [19] or experimentally determined by measuring the standard deviation of a cluster of localizations originating from a single fluorophore [3], the effects of labeling density and probe size can be challenging to determine. One strategy to quantify the overall resolution is to measure the separation distance between two closely spaced, barely resolvable structures in the image (e.g. the two walls of a hollow microtubule) [15,22]. However, finding such structures in a given image is difficult. Recently, a non-biased method based on Fourier ring correlation (FRC), originally developed for electron microscopy of single proteins [23], has been applied to super-resolution to calculate "intrinsic" image resolution directly from experimental data [24,25]. This method works by splitting the single-molecule localization data into two statistically independent sets to generate two sub-images. The Fourier transform of the two sub-images is then computed and correlated and the largest spatial frequency for which the correlation is still considerable is taken as a measure of the resolution. The inverse of this spatial frequency is the spatial resolution limit below which two objects cannot be resolved. In addition, FRC can also be used to estimate the average number of times a single emitter is localized, therefore helping to reduce over-counting artefacts (see below).

Spatial organization and molecular counting

In single molecule localization microscopy, super-resolution images are built molecule by molecule. Therefore, in principle, the imaging strategy should allow determining absolute numbers of molecules that exist in specific sub-cellular compartments. However, it is important to carefully examine how many molecules are missed or falsely included into the analysis.

Artificial clustering and over-counting

Artificial clustering and over-counting can arise due to several reasons. For example, if polyclonal primary and/or secondary antibodies are used, multiple antibodies can bind to the same protein giving rise to over-labeling. Antibodies can also physically crosslink proteins, leading to artificial clustering. Nonetheless, antibody labeling has been used to determine the relative amount and heterogeneity of synaptic proteins inside individual synapses using super-resolution imaging [26]. For determining absolute protein stoichiometry and sub-cellular protein distribution, fluorescent proteins that allow one-to-one tagging of the protein of interest may be preferable. Among these fluorescent proteins, irreversibly photoactivatable and photoconvertible ones are the best candidates for quantitative imaging, since in principle each fluorescent protein is imaged (and counted) only once. However, even the irreversible fluorescent proteins undergo transitions to non-fluorescent off states (blinking and re-activation) and can reappear multiple times during the imaging [27]. If not taken into account, this effect gives rise to over-counting and may make the image look clustered while there is no actual physical clustering of the target.

One way to account for intermittency of fluorescent protein emission is to take advantage of the time dependence of the blinking and photoactivation [28-30] (**Figure 1**). Typically, if the photoactivation is carried out slowly over a long time [30], blinking (or re-activation) events are closer in time compared to the photoactivation of a new fluorescent protein (**Figure 1b and c**). Therefore, peaks (or localizations) due to blinking can be grouped together based on a minimum dark time or cutoff time (τ_{cuttof}). In this case, only localizations appearing after a time larger than τ_{cuttof} are considered to arise from a new fluorescent protein (**Figure 1d**). τ_{cuttof} can be determined experimentally, by imaging purified fluorescent proteins on glass. When the density of the proteins to be counted is very high, the probability of photoactivation increases and blinking and new photoactivations start overlapping in time, making counting more challenging. Therefore, fluorescent proteins with low blinking (and re-activation) rates and short blinking times are preferable (e.g. Dendra2 and PA-mCherry) [30,31]. In addition, instead of using a single value, τ_{cuttof} can be characterized as a function of protein density. An algorithm can then be used that starts with an initial value of τ_{cuttof} set to zero, counts the number of molecules and adjusts the value of τ_{cuttof} based on this number iteratively until it converges [30]. The dark time analysis has mostly been applied to super-resolution images of fluorescent proteins, since the photophysics of most small organic fluorophores (e.g. AlexaFluor647) are more complex and do not allow spatiotemporal grouping of localizations. However, recently, Zhao et al. demonstrated that the blinking events of rhodamine dyes are also temporally grouped [32]. Therefore, using genetically encoded SNAP and Halo tags to link these dyes to RNA polymerase II, they could determine the spatial organization and stoichiometry of this motor inside the nucleus.

Statistical analysis such as pair-correlation functions can also be used to correct for over-counting and artificial clustering to determine the true spatial organization of proteins and count their numbers [33-35] (**Figure 2**). Pair correlation function reports the probability to find a second localization a distance r away from a given localization. It is given by the sum of correlations arising from multiple appearances of the same probe and the correlations due to the spatial distribution of labeled proteins. Therefore, if the first contribution is known, it can be used to correct the experimental data for over-counting and determine the true spatial distribution of proteins of interest. The correlations arising from multiple appearances of the same probe can be computed by using a calibration sample in which the probe is randomly distributed on a glass slide and imaged under the same experimental conditions (**Figure 2a-c**). In the absence of blinking (and re-activation) the correlation curve for the calibration sample should be flat with a value of one, consistent with random distribution of the fluorescent protein on the glass slide. Blinking and re-activation leads to higher correlations at small length scales (comparable to the localization precision), which must be corrected for in the experimental data. After this correction, the decay of the remaining correlation curve is a measure of the spatial extend of clustering (cluster size) and the amplitude of the correlation curve is related to the number of proteins within a cluster (**Figure 2d-f**). This type of analysis can also be applied to two-color images to determine the level of co-localization of multiple proteins. In this case, multiple appearance of the same probe does not influence the cross-correlation curve, making analysis and interpretation easier. Spatial co-organization and co-localization of proteins can also be quantified by

determining an "interaction potential" that is most likely to lead to the observed distribution of point localizations [36,37].

Finally, the FRC analysis described above [24] can also be used to extract the average number of times a molecule blinks given that the emitter activation follows a known distribution (e.g. Poisson statistics when not limited by photobleaching). For intermediate spatial frequencies, the influence of multiple localizations of the same emitter dominates the cross-correlation. If the decay of the correlation in this regime is fitted, the over-counting due to intermittency can be accounted for without the need for a calibration sample.

Missed molecules and under-counting

Once the effects of blinking and re-activation are corrected, the remaining number of localizations is a measure of the detected number of probes. However, many complications remain in converting this number to actual biological stoichiometry.

First, it is important that there is a one-to-one ratio between the protein of interest and the label. It is often challenging to achieve this one-to-one ratio with antibodies. While polyclonal antibodies can lead to overlabeling, the large size of the antibody can also lead to underlabeling due to steric hindrance. In practice, determining the labeling efficiency of an antibody is quite challenging and smaller probes such as aptamers and nanobodies have been demonstrated to lead to denser labeling of certain targets and higher spatial resolution in super-resolution images [38,39]. In principle, fluorescent proteins avoid this complication, giving rise to a one-to-one labeling ratio; however, the expression strategy used can cause additional problems. Transient transfection, the most common way of tagging proteins with fluorescent proteins in mammalian cells, leads to a mixture of endogenous unlabeled and over-expressed labeled protein. Ideally, one would like to determine the stoichiometry and spatial distribution of endogenous and not overexpressed proteins. With advances in genome editing, it is now possible to endogenously tag target proteins with fluorescent proteins [40,41].

Second, the imaging strategy must be such that multiple probes are not photoactivated simultaneously within a diffraction limited volume, since their images will overlap leading to missed events. The number of photoactivated probes is proportional to the power of the photoactivation laser and the total number of the remaining un-activated probes. Therefore, an imaging strategy must be followed in which the power of the photoactivation laser starts out very low and is progressively and slowly increased over time [30,42]. Similarly, the imaging period must be long enough such that all the probes are exhaustively imaged. Plotting a cumulative curve of localized molecules in each frame can give an indication of whether this condition has been satisfied [42]. The cumulative curve should increase slowly, reaching a plateau once most of the probes have been imaged.

Last but not least, failed photoactivation can lead to missed events and undercounting. A number of recent papers have used calibration standards to calculate the percentage of successful photoactivation during super-resolution imaging for a number of fluorescent proteins [31,43,44]. Durisic et al. took advantage of an *in vivo* "nanotemplate" with a well-

defined subunit stoichiometry, the human glycine receptor (GlyR) [31] (**Figure 3**). When expressed in Xenopus oocytes, which do not endogenously express this receptor, GlyR forms hetero-pentameric ion channels with three α- and two β-subunits [45]. The known stoichiometry made it possible to use binomial statistics to characterize fluorescent protein photoactivation efficiency by counting "steps" in single-step photobleaching or "peaks" in super-resolution intensity-time traces. Similarly, generating tandem repeats of fluorescent proteins attached to membrane proteins [44] or cytoplasmically expressing these tandem repeats at very low densities [43] allowed the use of binomial statistics to characterize the percentage of photoactivation. These results have shown that typically only 50-60% of fluorescent proteins are actually photoactivated into a fluorescent form and this number must be taken into account as a correction factor to properly count proteins in super-resolution images.

Conclusions and Outlook

Enormous amount of progress has been made in recent years in the field of super-resolution microscopy. New imaging methods with different capabilities (3D, multi-color) and new analysis methods to reconstruct super-resolution images from raw data and extract quantitative information have been developed. While the photophysical properties of the probes, labeling and imaging strategies make image analysis complex, with adequate care, it is possible to measure protein stoichiometry (multimeric, dimeric or oligomeric) [43,46], count protein numbers [30,42,44,47,48] and characterize the spatial nano-organization of proteins [33,49]. A number of open-source (typically ImageJ-based) software is now available for biologists who wish to quantify their super-resolution images [24,37]. As the field moves forward, researchers will greatly benefit from the development of new probes or identification of buffer and imaging conditions that lead to high photon outputs, high photoactivation efficiencies and low blinking or re-activation rates.

Figure Captions

Figure 1: Dark time analysis and spatiotemporal grouping of localizations: (a) PALM image of a HeLa cell expressing SrcN15-mEos2 as a negative clustering control. (b) Plot of localizations color-coded in time. Mono-chromatic clusters are indicative of artificial clustering due to the reappearance of the same mEos2 molecule multiple times. (c) Kymograph of the spatial clusters also confirms that the localizations are clustered in time. (d-e) Setting τ_{cuttof} = 10 seconds and grouping localizations that appear in time intervals shorter than τ_{cuttof} removes artificial clustering. (f) PALM image of a HeLa cell expressing β2-AR-mEos2 as a positive control of clustering. (g-h) Spatial clusters remain even after setting τ_{cuttof} = 10 seconds as expected. Reproduced with permission from reference 27.

Figure 2: Pair correlation analysis to identify spatial organization of proteins: (a) Calibration sample consisting of purified fluorescent protein randomly immobilized on glass slide. (b) PALM image of the calibration sample (PA-GFP). (c) Pair-correlation analysis to determine and correct for the contribution from multiple appearances of the same fluorescent protein (blue curve). (d-f) Application of pair correlation analysis to the PALM image of membrane proteins (red curve is before correction, blue curve is the contribution from multiple appearances of the same fluorescent protein and green curve is after correction for this effect). Reproduced with permission from reference 33.

Figure 3: Determination of fluorescent protein photoactivation (PA) efficiency using calibration samples: Drawing of the human glycine receptor (GlyR) with fluorescent protein tagged β- and untagged α-subunit expressed in Xenopus oocyte membrane is shown. The green fluorescent protein refers to the native form of a photoconvertible fluorescent protein (e.g. mEos2) and the red fluorescent protein refers to the photoconverted form. Single step-photobleaching intensity-time traces can be obtained after photoconversion of the fluorescent proteins. Alternatively, the fluorescent proteins can be imaged with PALM to generate intensity-time traces containing peaks. Steps or peaks in intensity-time traces are counted; sufficient statistics are built and fit to the binomial distribution to obtain the photoactivation efficiency. Shown is the photoactivation efficiency of mEos2 (red curve) as a function of illumination time by 405 nm laser light to induce photoactivation. For more details, see reference 30.

References

1. Klar TA, Jakobs S, Dyba M, Egner A, Hell SW: Fluorescence microscopy with diffraction resolution barrier broken by stimulated emission. *Proc Natl Acad Sci U S A* 2000, 97:8206-8210.
2. Gustafsson MG: Nonlinear structured-illumination microscopy: wide-field fluorescence imaging with theoretically unlimited resolution. *Proc Natl Acad Sci U S A* 2005, 102:13081-13086.
3. Rust MJ, Bates M, Zhuang X: Sub-diffraction-limit imaging by stochastic optical reconstruction microscopy (STORM). *Nat Methods* 2006, 3:793-795.
4. Betzig E, Patterson GH, Sougrat R, Lindwasser OW, Olenych S, Bonifacino JS, Davidson MW, Lippincott-Schwartz J, Hess HF: Imaging intracellular fluorescent proteins at nanometer resolution. *Science* 2006, 313:1642-1645.
5. Hess ST, Girirajan TP, Mason MD: Ultra-high resolution imaging by fluorescence photoactivation localization microscopy. *Biophys J* 2006, 91:4258-4272.
6. Heilemann M: Fluorescence microscopy beyond the diffraction limit. *J Biotechnol* 2010, 149:243-251.
7. Huang B, Babcock H, Zhuang X: Breaking the diffraction barrier: super-resolution imaging of cells. *Cell* 2010, 143:1047-1058.
8. Patterson G, Davidson M, Manley S, Lippincott-Schwartz J: Superresolution imaging using single-molecule localization. *Annu Rev Phys Chem* 2010, 61:345-367.
9. Thompson RE, Larson DR, Webb WW: Precise nanometer localization analysis for individual fluorescent probes. *Biophys J* 2002, 82:2775-2783.
10. Patterson GH, Lippincott-Schwartz J: A photoactivatable GFP for selective photolabeling of proteins and cells. *Science* 2002, 297:1873-1877.
11. Bates M, Blosser TR, Zhuang X: Short-range spectroscopic ruler based on a single-molecule optical switch. *Phys Rev Lett* 2005, 94:108101.
12. Heilemann M, Margeat E, Kasper R, Sauer M, Tinnefeld P: Carbocyanine dyes as efficient reversible single-molecule optical switch. *J Am Chem Soc* 2005, 127:3801-3806.
13. Fernandez-Suarez M, Ting AY: Fluorescent probes for super-resolution imaging in living cells. *Nat Rev Mol Cell Biol* 2008, 9:929-943.
14. Lippincott-Schwartz J, Patterson GH: Photoactivatable fluorescent proteins for diffraction-limited and super-resolution imaging. *Trends Cell Biol* 2009, 19:555-565.
15. Dempsey GT, Vaughan JC, Chen KH, Bates M, Zhuang X: Evaluation of fluorophores for optimal performance in localization-based super-resolution imaging. *Nat Methods* 2011, 8:1027-1036.
16. Habuchi S, Ando R, Dedecker P, Verheijen W, Mizuno H, Miyawaki A, Hofkens J: Reversible single-molecule photoswitching in the GFP-like fluorescent protein Dronpa. *Proc Natl Acad Sci U S A* 2005, 102:9511-9516.
17. Wiedenmann J, Ivanchenko S, Oswald F, Schmitt F, Rocker C, Salih A, Spindler KD, Nienhaus GU: EosFP, a fluorescent marker protein with UV-inducible green-to-red fluorescence conversion. *Proc Natl Acad Sci U S A* 2004, 101:15905-15910.
18. Mortensen KI, Churchman LS, Spudich JA, Flyvbjerg H: Optimized localization analysis for single-molecule tracking and super-resolution microscopy. *Nat Methods* 2010, 7:377-381.
19. Stallinga S, Rieger B: The effect of background on localization uncertainty in single emitter imaging. *IEEE Int Symp Biomedical Imaging* 2012:988-991.

20. Shroff H, Galbraith CG, Galbraith JA, Betzig E: Live-cell photoactivated localization microscopy of nanoscale adhesion dynamics. *Nat Methods* 2008, 5:417-423.

21. Lakadamyali M, Babcock H, Bates M, Zhuang X, Lichtman J: 3D Multicolor Super-Resolution Imaging Offers Improved Accuracy in Neuron Tracing. *PLoS One* 2012, 7:e30826.

22. Vaughan JC, Jia S, Zhuang X: Ultrabright photoactivatable fluorophores created by reductive caging. *Nat Methods* 2012, 9:1181-1184.

23. Saxton WO, Baumeister W: The correlation averaging of a regularly arranged bacterial cell envelope protein. *J Microsc* 1982, 127:127-138.

**24. Nieuwenhuizen RP, Lidke KA, Bates M, Puig DL, Grunwald D, Stallinga S, Rieger B: Measuring image resolution in optical nanoscopy. *Nat Methods* 2013, 10:557-562.

**25. Banterle N, Bui KH, Lemke EA, Beck M: Fourier ring correlation as a resolution criterion for super-resolution microscopy. *J Struct Biol* 2013, 183:363-367.

Ref 24 and 25 were published around the same time and they both independently develop Fourier Ring Correlation (FRC) analysis as a method to measure the intrinsic image resolution of super-resolution images without the need for calibration standards.

26. Dani A, Huang B, Bergan J, Dulac C, Zhuang X: Superresolution imaging of chemical synapses in the brain. *Neuron* 2010, 68:843-856.

27. Annibale P, Scarselli M, Kodiyan A, Radenovic A: Photoactivatable Fluorescent Protein mEos2 Displays Repeated Photoactivation after a Long-Lived Dark State in the Red Photoconverted Form. *Journal of Physical Chemistry Letters* 2010, 1:1506-1510.

**28. Annibale P, Vanni S, Scarselli M, Rothlisberger U, Radenovic A: Identification of clustering artifacts in photoactivated localization microscopy. *Nat Methods* 2011, 8:527-528.

**29. Annibale P, Vanni S, Scarselli M, Rothlisberger U, Radenovic A: Quantitative photo activated localization microscopy: unraveling the effects of photoblinking. *PLoS One* 2011, 6:e22678.

Ref 28 and 29 employ the concept of dark-time analysis to set a cut-off time in order to reduce overcounting and clustering artefacts that result from the re-apparence of the same probe multiple times in the image.

**30. Lee SH, Shin JY, Lee A, Bustamante C: Counting single photoactivatable fluorescent molecules by photoactivated localization microscopy (PALM). *Proc Natl Acad Sci U S A* 2012, 109:17436-17441.

Ref 30 extends the dark-time analysis to introduce a variable cut-off time that is dependent on protein density. It then develops an algorithm that varies the cut-off time based on the determined protein density in an iterative way for more accurate counting of proteins labeled with "irreversible switching" flurescent proteins.

**31. Durisic N, Laparra-Cuervo L, Sandoval-Alvarez A, Borbely JS, Lakadamyali M: Single-molecule evaluation of fluorescent protein photoactivation efficiency using an in vivo nanotemplate. *Nat Methods* 2014, 11: 156-162.

Ref 31 uses the human Glycine receptor as a nanotemplate of known stoichiometry to characterize the percentage of successful photoactivation (photoactivation efficiency) of eight irreversibly photoactivatable and photoconvertible fluorescent proteins used in single molecule counting.

32. Zhao ZW, Roy R, Gebhardt JC, Suter DM, Chapman AR, Xie XS: Spatial organization of RNA polymerase II inside a mammalian cell nucleus revealed by reflected light-sheet superresolution microscopy. *Proc Natl Acad Sci U S A* 2014, 111:681-686.

**33. Sengupta P, Jovanovic-Talisman T, Lippincott-Schwartz J: Quantifying spatial organization in point-localization superresolution images using pair correlation analysis. *Nat Protoc* 2013, 8:345-354.

**34. Sengupta P, Jovanovic-Talisman T, Skoko D, Renz M, Veatch SL, Lippincott-Schwartz J: Probing protein heterogeneity in the plasma membrane using PALM and pair correlation analysis. *Nat Methods* 2011, 8:969-975.

Ref 33 and 34 develop a statistical analysis method based on pair-correlation analysis to account for the effects of multiple reapparence of the same "irreversible switching" probe in super-resolution images and to determine the underlying molecular distribution and stoichiometry.

*35. Veatch SL, Machta BB, Shelby SA, Chiang EN, Holowka DA, Baird BA: Correlation functions quantify super-resolution images and estimate apparent clustering due to over-counting. *PLoS One* 2012, 7:e31457.

Ref 35 extends the concepts of pair-correlation analysis to reversibly switching probes and immuno-electron microscopy.
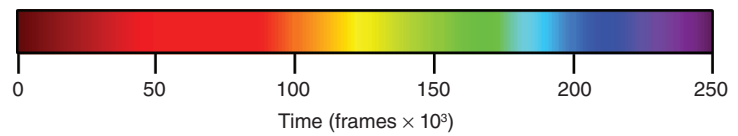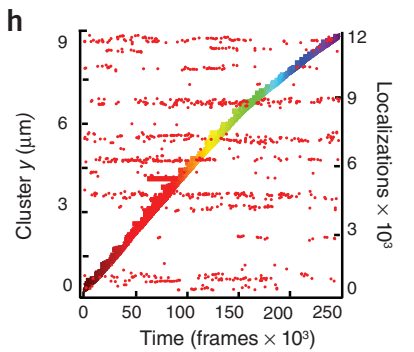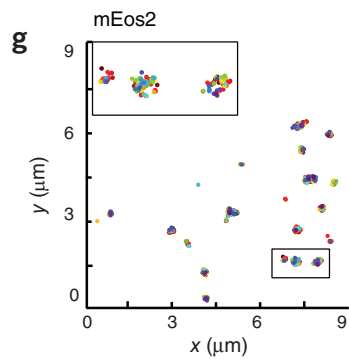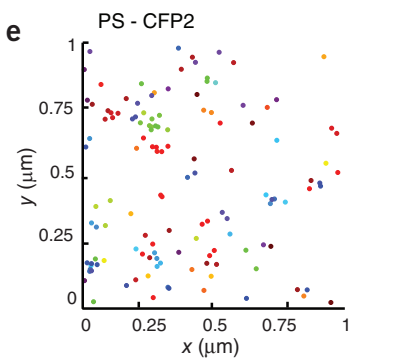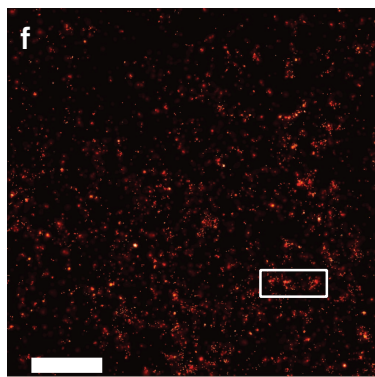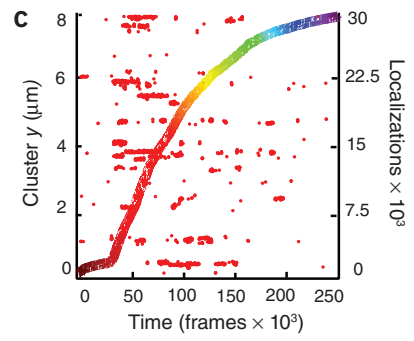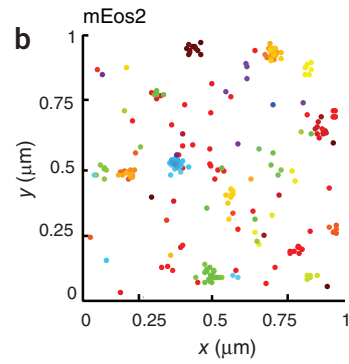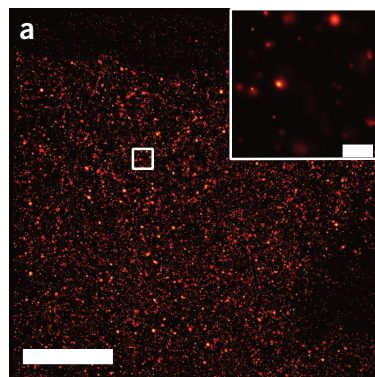
36. Helmuth JA, Paul G, Sbalzarini IF: Beyond co-localization: inferring spatial interactions between sub-cellular structures from microscopy images. *BMC Bioinformatics* 2010, 11:372.

37. Shivanandan A, Radenovic A, Sbalzarini IF: MosaicIA: an ImageJ/Fiji plugin for spatial pattern and interaction analysis. *BMC Bioinformatics* 2013, 14:349.

38. Opazo F, Levy M, Byrom M, Schafer C, Geisler C, Groemer TW, Ellington AD, Rizzoli SO: Aptamers as potential tools for super-resolution microscopy. *Nat Methods* 2012, 9:938-939.

39. Ries J, Kaplan C, Platonova E, Eghlidi H, Ewers H: A simple, versatile method for GFP-based super-resolution microscopy via nanobodies. *Nat Methods* 2012, 9:582-584.

40. Ran FA, Hsu PD, Wright J, Agarwala V, Scott DA, Zhang F: Genome engineering using the CRISPR-Cas9 system. *Nat Protoc* 2013, 8:2281-2308.

41. Wood AJ, Lo TW, Zeitler B, Pickle CS, Ralston EJ, Lee AH, Amora R, Miller JC, Leung E, Meng X, et al.: Targeted genome editing across species using ZFNs and TALENs. *Science* 2011, 333:307.

*42. Gunzenhauser J, Olivier N, Pengo T, Manley S: Quantitative super-resolution imaging reveals protein stoichiometry and nanoscale morphology of assembling HIV-Gag virions. *Nano Lett* 2012, 12:4705-4710.

Ref 42 develops a theoretical model to determine if all the probes have been exhaustively imaged at the end of a super-resolution imaging session and uses this concept to count Gag proteins during HIV assembly.
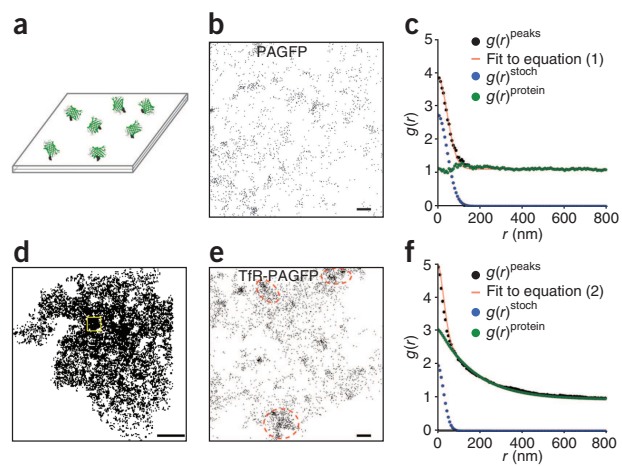
43. Nan X, Collisson EA, Lewis S, Huang J, Tamguney TM, Liphardt JT, McCormick F, Gray JW, Chu S: Single-molecule superresolution imaging allows quantitative analysis of RAF multimer formation and signaling. *Proc Natl Acad Sci U S A* 2013, 110:18519-18524.
**44. Puchner EM, Walter JM, Kasper R, Huang B, Lim WA: Counting molecules in single organelles with superresolution microscopy allows tracking of the endosome maturation trajectory. *Proc Natl Acad Sci U S A* 2013, 110:16015-16020.

Ref 44 uses tandem repeats of mEos2 as a calibration sample to account for the effects of overcounting (multiple reapparence of the same probe) and undercounting (failed photoactivation) to measure the changes to protein numbers on endosomes during endosome maturation.

45. Durisic N, Godin AG, Wever CM, Heyes CD, Lakadamyali M, Dent JA: Stoichiometry of the human glycine receptor revealed by direct subunit counting. *J Neurosci* 2012, 32:12915-12920.
46. Renz M, Daniels BR, Vamosi G, Arias IM, Lippincott-Schwartz J: Plasticity of the asialoglycoprotein receptor deciphered by ensemble FRET imaging and single-molecule counting PALM imaging. *Proc Natl Acad Sci U S A* 2012, 109:E2989-2997.
47. Lehmann M, Rocha S, Mangeat B, Blanchet F, Uji IH, Hofkens J, Piguet V: Quantitative multicolor super-resolution microscopy reveals tetherin HIV-1 interaction. *PLoS Pathog* 2011, 7:e1002456.
48. Lando D, Endesfelder U, Berger H, Subramanian L, Dunne PD, McColl J, Klenerman D, Carr AM, Sauer M, Allshire RC, et al.: Quantitative single-molecule microscopy reveals that CENP-A(Cnp1) deposition occurs during G2 in fission yeast. *Open Biol* 2012, 2:120078.
49. Scarselli M, Annibale P, Radenovic A: Cell type-specific beta2-adrenergic receptor clusters identified using photoactivated localization microscopy are not lipid raft related, but depend on actin cytoskeleton integrity. *J Biol Chem* 2012, 287:16768-16780.

Figure

Figure

Figure